

## Organic/Inorganic Hybrid Composite Films from Polyimide and Organosilica: Effect of the Type of Organosilica Precursors

Minsoo Son<sup>1</sup>, Sewon Han<sup>2</sup>, Donghee Han<sup>2</sup>, Youngkyoo Kim<sup>3</sup>, Jihan Lim<sup>1</sup>, Il Kim<sup>1</sup>, Chang-Sik Ha<sup>1</sup> (✉)

<sup>1</sup> Department of Polymer Science and Engineering, Pusan National University, Busan 609-735, South Korea

<sup>2</sup> Advanced Materials and Application Research Lab., Korea Electrotechnology Research Institute, P.O.Box 20, Changwon 641-600, South Korea

<sup>3</sup> Organic Nanoelectronics Laboratory, Department of Chemical Engineering, Kyungpook National University, Daegu 702-701, South Korea

E-mail: csha@pusan.ac.kr; Fax: +82-51-514-4331

Received: 30 August 2007 / Revised version: 2 November 2007 / Accepted: 16 January 2008

Published online: 31 January 2008 – © Springer-Verlag 2008

### Summary

We report the influence of the type of organosilica precursors on the growth of organosilica domains and the interfacial interaction between polyimide (PI) and organosilica in PI/organosilica hybrid composite films. The organosilica precursors used are tetraethoxysilane (TEOS), triethoxy(ethyl)silane (TEES), and 1,2-bis(triethoxysilyl)ethane (BTSE). The hybrid composite films were prepared by thermal imidization of the precursor films that were made via sol-gel process of the mixture of poly(4,4'-oxydianiline benzenetetracarboxylic acid) (PMDA-ODA PAA) and organosilica precursors. The hybrid composite films were characterized using Fourier transform infrared (FT-IR) spectra, <sup>29</sup>Si cross polarization (CP) MAS-NMR spectra, field emission-scanning electron microscopy (FE-SEM), UV-visible spectra, small angle x-ray scattering (SAXS), dynamic mechanical analysis (DMA), and thermogravimetric analysis (TGA). The results showed that the TEES precursor was more pronounced in improving the interaction of corresponding organosilica with PI than other precursors.

### Introduction

Organic/inorganic hybrid composites that utilize polymers as a matrix have been recognized as one of new class advanced materials, because they can take benefit by combining the merits of both inorganic materials (rigidity and thermal stability) and organic polymers (flexibility, ductility, and processability)<sup>1–9</sup>.

Among various polymers used for hybrid composites, aromatic polyimides (PI) have attracted keen interest because of the potential for use in microelectronics and aerospace industries due to their outstanding chemical, physical, thermal, and mechanical properties even at high temperatures.<sup>10,11</sup> In terms of inorganic materials

for hybrid composites, silica has been widely used owing to its low dielectric property and high thermal stability which are of importance for microelectronic applications.<sup>12</sup> It has been, indeed, reported that incorporating silica particles into a PI matrix was effective to enhance the mechanical and thermal properties of the PI film.<sup>12-14</sup>

For the preparation of PI/silica composite films various studies have been reported and most of them did employ a sol-gel process.<sup>15,16</sup> Typical sol-gel process provides *in-situ* generation of silica nanoparticles that are three-dimensionally crosslinked by the successive reactions of hydrolysis and polycondensation of their corresponding precursor molecules. Most widely used precursor of silica is tetraethoxysilane (TEOS).<sup>17,18</sup> The properties of resulting PI/silica hybrid composites are significantly influenced by various factors including pH, temperature, nature of solvent, kind of polymers, etc. When these factors are not optimally controlled, most of PI/silica hybrid films exhibit a large scale phase segregation that reduces the combined advantages of organic and inorganic constituents so that sometimes much worse properties than individual constituents can be obtained.

Therefore minimizing the degree of phase segregation is of utmost importance and can be achieved by a variety of methods as reported<sup>19</sup>: (1) introducing desirable functional groups to the each end of polymer chains, (2) selecting silica precursor having organic group, (3) incorporating comonomers that have suitable functional groups, and (4) adding a coupling agent to chemically bind between PI chains and silica.<sup>20</sup>

In this study, we attempt to improve the degree of phase segregation by differing kinds of silica precursors such as TEOS (as a control), triethoxy(ethyl)silane (TEES), and 1,2-bis(triethoxysilyl)ethane (BTSE). In more detail, we study the effect of inserted methylene group (-CH<sub>2</sub>-) into the silica precursors (see Figure 1). The resulting composite films were characterized by using various spectroscopic techniques and thermal/mechanical measurements.

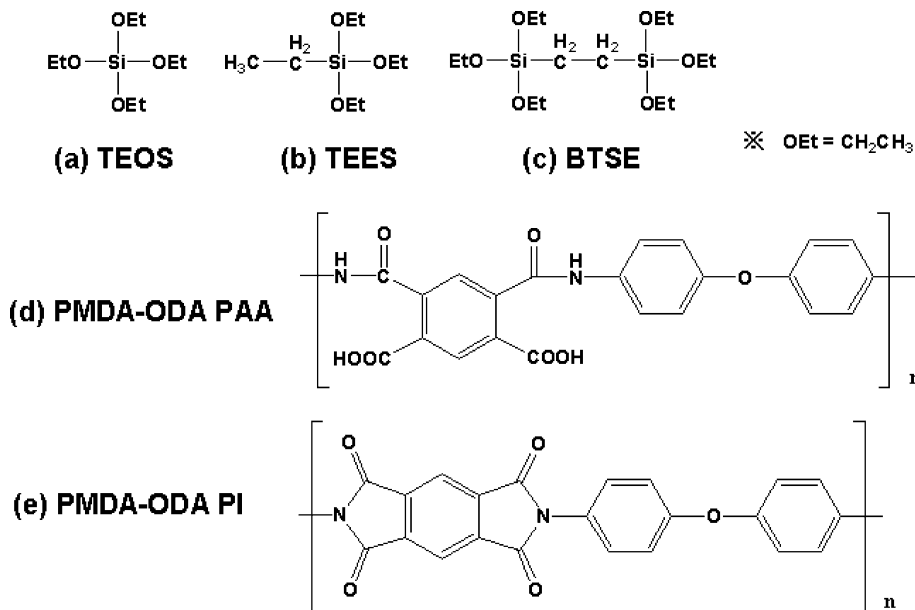


**Figure 1.** Chemical structure of (a) TEOS, (b) TEES, (c) BTSE, (d) PMDA-ODA PAA, (e) PMDA-ODA PI.

## Experimental part

### Materials

4,4'-oxydianiline (ODA, 97%), pyromellitic dianhydride (PMDA, 97%), N,N'-dimethylacetamide (DMAc, HPLC grade), tetraethylorthosilicate (TEOS, 98%), triethoxy(ethyl)silane (TEES, 96%), and 1,2-bis(triethoxysilyl)ethane (BTSE, 96%) were purchased from Aldrich and used as received.

### *Preparation of polyimide/organosilica hybrid films*

First, ODA (2.403g ; 12mmol) was added to DMAc (16.07ml) in a two-necked round-bottom flask under nitrogen atmosphere and stirred for 2 hr for complete dissolution. Next, PMDA (2.618g ; 12mmol) was added to the solution of ODA in DMAc. The reaction (polymerization) was carried out for 12hr at room temperature, leading to poly(4,4'-oxydianiline pyromellitic acid) (PMDA-ODA PAA) solution. To this PAA solution, corresponding amount of organosilica precursors was added and stirred for 30 min to obtain a homogeneous solution. Next, deionized water was dropped into the solution of PMDA-ODA PAA and organosilica precursor, and then stirred for 12 hr in order to complete the sol-gel reaction.

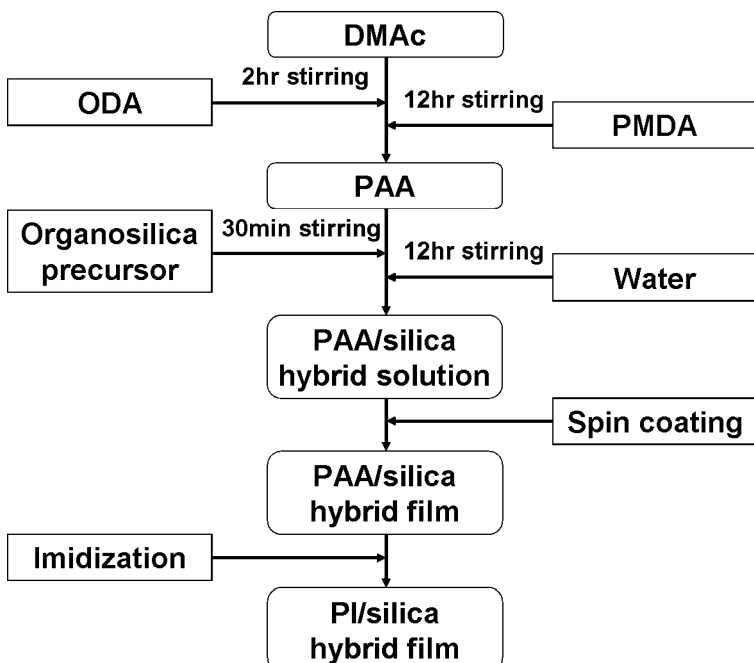


**Figure 2.** Schematic diagram for the preparation process of PMDA-ODA PI/organosilica hybrid films.

The mixture solution after sol-gel reaction was spin-coated onto a glass slide and then softbaked at 80°C for 6 hr. The solid concentration was fixed to 10 wt.% for all precursor solutions. These softbaked films (thickness = 90μm) were thermally

imidized by a stepwise imidization process under nitrogen atmosphere for 30 min at 140°C, 200°C, and 250°C: The heating rate employed was ~2°C/min, which resulted in the hybrid composite films of poly(4,4'-oxydianiline pyromellitimide) (PMDA-ODA PI) and organosilica. Figure 2 summarizes the whole process for the preparation of hybrid films. The chemical structure of PMDA-ODA PI is shown in Figure 1. Table 1 summarizes the detailed specification for the preparation of hybrid precursor films and the corresponding name of samples.

**Table 1.** Preparation of PAA, PAA/organosilica and hybrid films.

Sample code <sup>a</sup>	PAA + DMAc <sup>b</sup> (g)	TEOS (g)	TEES (g)	BTSE (g)	Organosilica precursor <sup>c</sup> (wt%)	Film state <sup>d</sup>
PI	8.0	-	-	-	-	T
T5	8.0	0.0421	-	-	5	T
T10	8.0	0.0889	-	-	10	T
T20	8.0	0.2000	-	-	20	O
S5	8.0	-	0.0421	-	5	T
S10	8.0	-	0.0889	-	10	T
S20	8.0	-	0.2000	-	20	T
E5	8.0	-	-	0.0421	5	T
E10	8.0	-	-	0.0889	10	T
E20	8.0	-	-	0.2000	20	O

<sup>a</sup> T5, T10, T20 : T series, S5, S10, S20 : S series, E5, E10, E20 : E series

<sup>b</sup> Weight of PAA+DMAc (=1 : 9) solution

<sup>c</sup> Organosilica precursor content (wt%) in PAA/organosilica hybrid

<sup>d</sup> Film state of PI and PI/silica hybrid films : T; Transparent, O; Opaque

### Measurements

Fourier transform Infrared (FT-IR) spectra of films were measured using a spectrometer (React IR™ 1000, Applied System, ASi). Interferogram spectra were collected between 400 and 4000 cm<sup>-1</sup> at a resolution of 4cm<sup>-1</sup>: 128 scans were taken. <sup>29</sup>Si cross polarization MAS NMR spectra (<sup>29</sup>Si CP/MAS NMR spectra) were obtained using a spectrometer (Bruker DSX400) with a 4 mm zirconia rotor spinning at 6 kHz (resonance frequencies: 79.5 MHz; 90° pulse widths: 5 µs; contact times: 2 ms; recycle delay : 3 s) at room temperature. The morphology of the fractured surfaces of the hybrid films were measured using a field emission-scanning electron microscopy (FE-SEM, JSM-6700F) with an acceleration voltage of 15 kV. UV-visible spectra were obtained using a spectrophotometer (U-2010, HITACHI) at room temperature. Small angle x-ray scattering (SAXS) patterns were measured using a synchrotron x-ray source of Pohang accelerator laboratory (PAL, South Korea): Co-K<sub>α</sub> ( $\lambda=1.608\text{ \AA}$ ) radiation with an energy range of 4~16keV (energy resolution ( $\Delta E/E$ ) =  $5\times 10^{-4}$ ; photon flux =  $10^{10}\text{--}10^{11}$  ph./s; beam size = 1 mm<sup>2</sup>). The SAXS scan range was fixed as  $0.0012\text{ nm}^{-1} < q < 0.3316\text{ nm}^{-1}$ . The thermomechanical property of hybrid films were performed using a dynamic mechanical analyzer (DMA, Q800, TA Instrument) (sample length = 2.5 cm; sample width = 0.5 cm; heating rate = 5°C/min; frequency = 3 Hz). The thermal stability of hybrid films was measured using a thermogravimetric analyzer (TGA, Q50, TA Instrument) (heating rate = 10°C/min; scan range = 40°C ~ 900°C).

## Results and Discussion

### *Examination of imidization and organosilica formation*

Prior to the detailed study of hybrid films, we examined the FT-IR spectra of pristine PMDA-ODA PAA and PMDA-ODA PI films in order to confirm the proper synthesis of precursor polymer and resulting polyimide (see Figure 3). The PMDA-ODA PAA film shows the characteristic peaks at around  $1650\text{ cm}^{-1}$  (carboxylic acid C=O vibration by the formation of amic acid),  $2820\text{ cm}^{-1}$  (carboxylic acid O-H vibration), and  $3410\text{ cm}^{-1}$  (amide N-H group vibration). The PMDA-ODA PI film shows the characteristic peaks at  $1710$  and  $1770\text{ cm}^{-1}$ , which correspond to both symmetric and asymmetric C=O stretching of imide group. Additionally the bands at  $1370$  and  $737\text{ cm}^{-1}$  are attributed to the formation of C-N stretching and imide ring deformation, while the band at  $1497\text{ cm}^{-1}$  is assigned to the vibration of benzene ring in the polyimide. The band at  $1173\text{ cm}^{-1}$  is attributed to the aromatic C<sub>6</sub>H<sub>4</sub> or C<sub>6</sub>H<sub>2</sub>. The peak at  $677\text{ cm}^{-1}$  is assumed to originate from the C-C=O in-plane swing vibration.

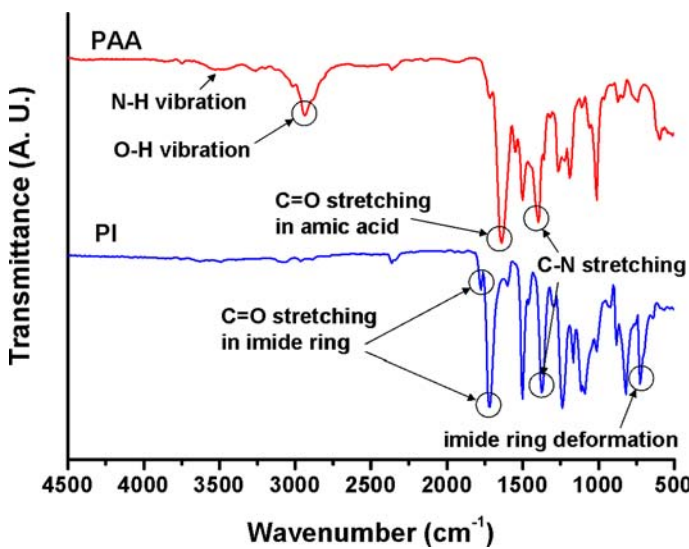


**Figure 3.** IR spectra of pristine PMDA-ODA PAA and PI.

The extent of thermal imidization in films was verified from both the disappearance of the band at  $1650\text{ cm}^{-1}$  and the growth of the imide group at  $1710\text{ cm}^{-1}$ . Figure 4 shows the normalized (around the wavenumbers between  $900\text{ cm}^{-1}$  and  $1300\text{ cm}^{-1}$ ) IR spectra of PMDA-ODA PI/organosilica hybrid films. The intensity of a weak band at  $1019\text{ cm}^{-1}$  that corresponds to the vibration of silica networks (Si-O-Si) gradually increases with increasing organosilica contents regardless of the kind of organosilica precursors. This indicates that three-dimensional Si-O-Si network was obviously made in the polyimide/organosilica hybrid films. This result is in good agreement with the earlier studies for the PI/silica hybrids.<sup>8,12,13,19,21-23</sup>

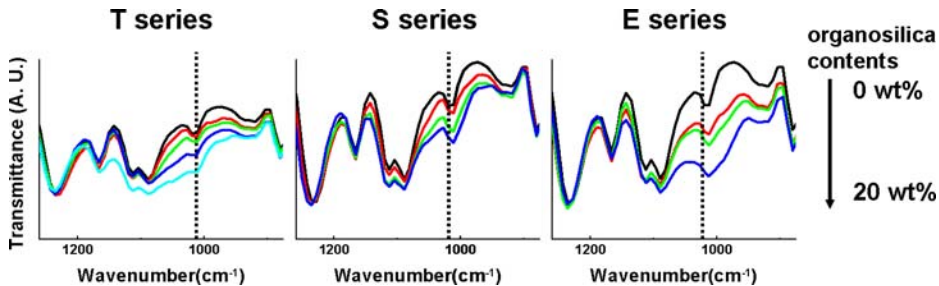


**Figure 4.** Normalized (around the wavenumbers between  $900\text{ cm}^{-1}$  and  $1300\text{ cm}^{-1}$ ) IR spectra of PMDA-ODA PI/organosilica hybrid films. For sample notations, see Table 1.

#### Investigation of Si-O-Si and Si-C bond features

We examined the status of Si–C bonding in organosilica domains by using  $^{29}\text{Si}$  CP/MAS NMR spectroscopy measurements.<sup>14,24–26</sup> As shown in Figure 5, the S20 and E20 hybrid films show only  $\text{T}^{\text{i}}$  peaks, whilst only  $\text{Q}^{\text{i}}$  peaks are detected for the T20 hybrid film. In more detail the T20 film shows three peaks at  $-92.0$ ,  $-100.0$  and  $-110.0\text{ ppm}$  with the fraction of  $14.4\%$ ,  $69.4\%$  and  $16.2\%$ , respectively, which can be assigned to  $\text{Q}^2$   $(\text{OH})_2\text{Si(OSi)}_2$ ,  $\text{Q}^3$   $(\text{OH})\text{Si(OSi)}_3$  and  $\text{Q}^4$   $\text{Si(OSi)}_4$ .<sup>14</sup> This result indicates that the partially uncondensed silanol groups were remained in the organosilicas in the hybrid films.

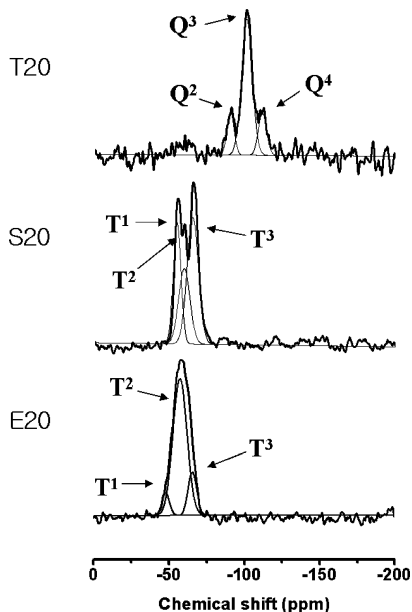


**Figure 5.**  $^{29}\text{Si}$  CP/MAS NMR spectra of PMDA-ODA PI/organosilica hybrid films. For sample notations, see Table 1.

Both S20 and E20 hybrid films exhibit three peaks at  $-48.0$ ,  $-57.0$  and  $-66.0\text{ ppm}$ , which can be assigned to  $\text{T}^1$   $\text{C(OH)}_2\text{Si(OSi)}$ ,  $\text{T}^2$   $\text{C(OH)}\text{Si(OSi)}_2$ , and  $\text{T}^3$   $\text{CSi(OSi)}_3$ ,

respectively.<sup>14,24-26</sup> We note that the fractions of the three T<sup>i</sup> signals obtained from the fitted curves are different because of the different chemical structure between TEES and BTSE (note that TEES has three ethoxy groups with one ethylene end group but BTSE has six ethoxy end groups): 28.8% (T<sup>1</sup>), 26.3% (T<sup>2</sup>), and 44.9% (T<sup>3</sup>) for S20; 7.0% (T<sup>1</sup>), 77.6% (T<sup>2</sup>), and 15.4% (T<sup>3</sup>) for E20. It is noteworthy that the fraction of T<sup>2</sup> is higher than that of T<sup>1</sup> and T<sup>3</sup> for E20, whereas the fraction of T<sup>1</sup> and T<sup>3</sup> is higher than that of T<sup>2</sup> for S20. This result discloses that TEES is mainly converted to completely 3-handed network organosilica particles with some uncondensed silanol (Si-OH) group residues, whereas BTSE leads to imperfectly networked organosilica particles that contain silanol groups (i.e., incomplete reaction). However, we note that Q<sup>i</sup> peaks, which are related to the purely hydrolyzed and/or completely condensed silica particles without any Si-C bonds, were not observed for both E20 and S20 hybrid films.

#### *Morphology of hybrid films*

As shown in the FE-SEM images (see Figure 6), the size of organosilica particles is 200~250 nm (T20), 500~700 nm (E20), and <60 nm (S20), respectively. This indicates that the particle size decreases with the number of ethoxy groups of organosilica precursors even though their relationship is not proportional. In particular, the huge difference in the film morphology between S20 and other precursors may talk an

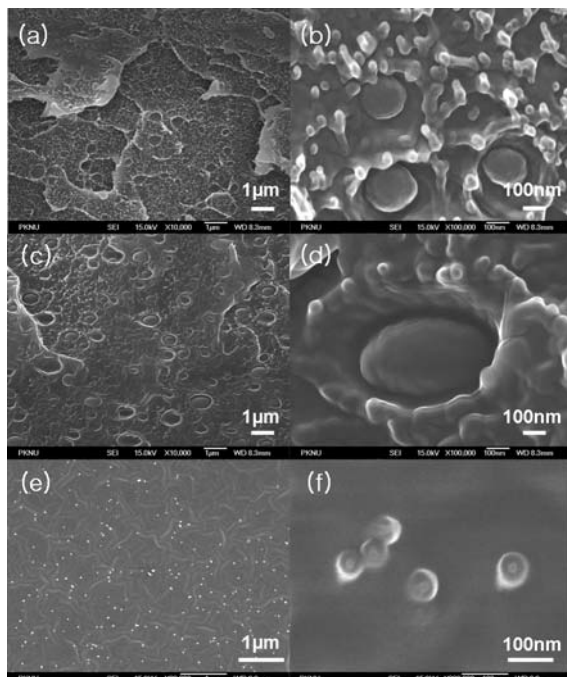


**Figure 6.** Fractured surface morphology of hybrid composite films (a), (b): T20, (c), (d): E20, (e), (f): S20. For sample notations, see Table 1; (a), (c), and (e) are in low magnification ((a), (c): x10,000, (e): x20,000); (b), (d), and (e) are in high magnification ((b), (d): x100,000, (f): x200,000).

importance of appropriate fractions of ethyl and ethoxy groups.<sup>13</sup> In other words too many ethoxy groups (more than three functionality in TEOS and BTSE) might give considerably fast rate of hydrolysis reaction which leads to the fast growth of silica particles. Thus the presence of one terminal ethyl group, instead of all four or more ethoxy groups, may help better interaction between organosilica particles and polyimide matrix.

#### *Optical property of hybrid films*

First we note that the hybrid films were too thick (100  $\mu\text{m}$ ) so that the transmittance below the wavelength of  $\sim 500$  nm was cut off for all samples (see Figure 7). Most of hybrid films, except T20 and E20, were optically transparent while the transmittance was decreased with increasing the content of organosilica precursors. This normal transparency is attributed to the size of organosilica particles which is less than the wavelength of visible light so that the light scattering loss is minimized.<sup>27</sup> However, in case of T20 and E20, corresponding hybrid films were opaque because of the bigger silica particles with increasing precursor contents (The transmittance of S20 at the wavelength of 550 nm was over 55 % but those of T20 and E20 are less than 8 %). In case of S series, even though the content of organosilica precursor becomes higher, superior transparency was achieved compared to T and E series, which is due to the better interaction between organosilica particles and PMDA-ODA PI.

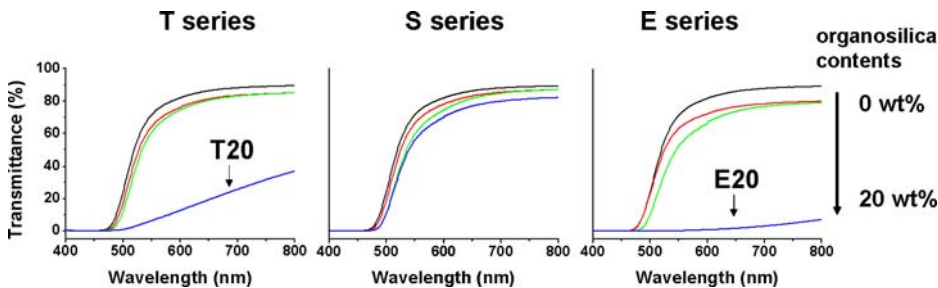


**Figure 7.** UV-visible spectra of PMDA-ODA PI and PI/organosilica hybrid films. For sample notations, see Table 1.

#### *Nanostructure of hybrid films*

Figure 8 shows the Lorentz-corrected SAXS patterns.<sup>28-30</sup> All films show a broad SAXS peak at  $0.05 < q < 0.15 \text{ \AA}^{-1}$  which is attributed to the mean long period of PMDA-ODA PI (ca. 66  $\text{\AA}$  for pristine film).<sup>31</sup> Although the size and distribution of organosilica particles formed in the hybrid films were not quantitatively examined, these SAXS results indicate that various sized organosilica particles were made during sol-gel process and they had an influence on the mean long period of the polyimide.<sup>25</sup> Here the long period of PI/organosilica hybrid films is smaller than that of the pristine PI. Basically the reduced long period can be attributed to the decreased size of crystal or phase domains. In particular, the intensity of scattering peaks at  $q=\sim 0.10 \text{ \AA}^{-1}$  was increased with increasing the content of TEES, whereas such increase was small for both T and E series. More interestingly no scattering peaks are observed below  $q=0.03 \text{ \AA}^{-1}$  for S series, whereas for both T and E series the intensity of the scattering peaks increases with increasing the content of organosilica in the hybrid films. This

trend is more pronounced for T series rather than E series. Since the particles measured at  $q=0.03 \text{ \AA}^{-1}$  have the average size of  $>210 \text{ \AA}$ , these SAXS patterns are in good agreement with the FE-SEM results which did indicate that the S series hybrid films exhibited better interfacial interaction than both T and E series hybrids.

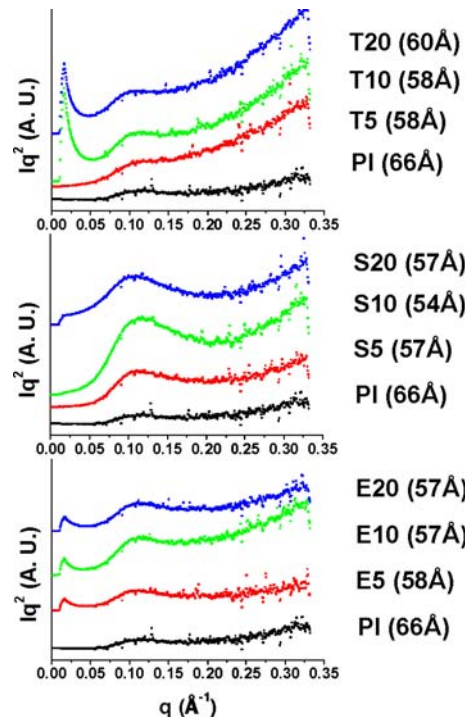


**Figure 8.** Lorentz-corrected SAXS patterns of pristine PMDA-ODA PI and hybrid films. For sample notations, see Table 1.

#### *Thermal stability and thermomechanical property*

Figure 9 shows the TGA and differential thermogravimetric (DTG) curves of pure PI and hybrid composite films with various organosilica contents (E series). The TGA

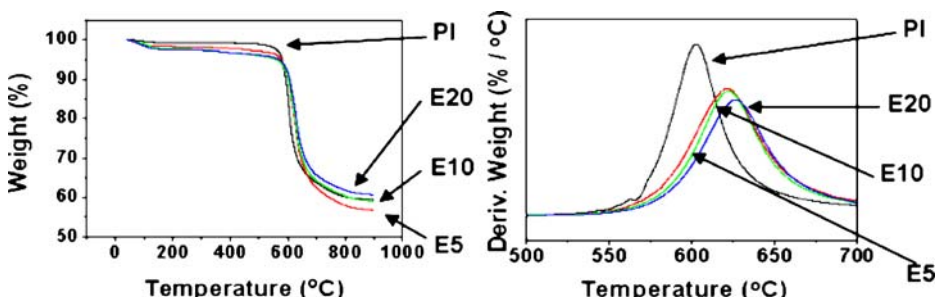


**Figure 9.** Thermogravity analysis (TGA) and differential thermogravimetric (DTG) curve of pristine PI, E5, E10, E20. For sample notations, see Table 1.

curves of hybrid films show that the weight loss initialized even below 100°C, which is attributed to the outgas of water molecules from further reaction of unreacted silanols upon heating. In particular, we find that the DTG curves do shift to the high temperature direction with increasing organosilica contents. This indicates that the thermal stability of hybrid films is improved in comparison to the pristine PI. We note that other organosilica precursors showed similar behavior to E series. Table 2 summarizes key parameters.

**Table 2.** Thermomechanical properties of PMDA-ODA PI and PI/organosilica hybrid films.

Sample code	Td <sup>a</sup> (°C)	Residue <sup>b</sup> (%)	Tg <sup>c</sup> (°C)	Storage modulus <sup>d</sup> (MPa)
PI	592.8	59.4	375.9	2816.8
T5	602.6	54.9	378.6	2643.3
T10	618.4	57.2	378.9	3214.8
T20	603.1	58.0	377.7	3197.5
S5	601.2	54.5	372.4	2715.4
S10	604.7	57.6	367.8	2964.2
S20	599.3	58.1	368.0	3048.2
E5	601.5	56.7	378.1	2783.4
E10	601.7	59.0	378.6	2897.5
E20	605.9	60.6	379.0	3261.7

<sup>a</sup> Thermal decomposition temperature corresponding to 10% weight loss.

<sup>b</sup> Residual ash at 900°C from TGA results.

<sup>c-e</sup> Tg and storage modulus determined by DMA measurements conducted with a heating rate of 5°C/min at 3 Hz.

<sup>d</sup> Storage modulus corresponding to 30°C.

As shown in Table 2, the storage modulus of hybrid composite films increased with the content of organosilica.<sup>32,33</sup> The glass transition temperature (Tg) of hybrid composite films was slightly increased with increasing the organosilica contents regardless of the kind of organosilica. Unexpectedly, however, the hybrid composite films from S series exhibit slightly lower Tg than the pristine PI and other hybrid films in spite of the better interaction between PI and corresponding organosilica.

## Conclusion

In this work we have discussed the influence of the type of organosilica precursors on the formation and property of PI/silica hybrid composite films. The FT-IR spectra did confirm the proper synthesis and preparation of polyimide and hybrid films. The <sup>29</sup>Si-NMR result showed that silica networks were formed but the TEES-based organosilica does limit the growth of organosilica particles due to the steric hindrance effect of ethyl moieties. The FE-SEM measurement showed that the TEES precursor delivers better interaction between PI matrix and organosilica. The hybrid composite films of T20 and E20 were opaque because these films had bigger size organosilica particles due to the over 4 ethoxy groups that play a critical role in increasing the (networking) reaction rate. The long period of polyimide (PMDA-ODA PI) was

affected by the presence of organosilica in hybrid films, while at higher organosilica contents the generated silica particles were bigger than those at lower organosilica content. The thermal property of hybrid composite films was generally improved by introducing organosilica particles, except the Tg trend of PI/TEES hybrid films.

*Acknowledgements.* The work was supported by the Korea Science and Engineering Foundation (KOSEF) through the National Research Laboratory Program funded by the Ministry of Science and Technology (MOST; M10300000369-06J0000-36910), the SRC / ERC Program of MOST / KOSEF (grant # R11-2000-070-080020), the Brain Korea 21 Project, and the Korea Electrotechnology Research Institute. We also thank the Pohang Accelerator Laboratory, Korea for SAXS measurements.

## References

1. Seino H, Mochizuki A, Ueda M, (1999) *J Polym Chem* 37 : 3584
2. Hedrick JL, Cha HJ, Miller RD, Yoon DY, Brown HR, Srinivasan S, Di Pietro R, (1997) *Macromolecules* 30 : 8512
3. Ha CS, Cho WJ, (2000) *Polym Adv Technol* 11 : 145
4. Huang JC, He CB, Xiao Y, Mya KY, Dai J, Siow YP, (2003) *Polymer* 44 : 4491
5. Wu KH, Chang TC, Yang JC, Chen HB, (2001) *J Appl Polym Sci* 79 : 965
6. XD, Zhong ZX, Jin G, (2006) *Macromol Res* 14(3) : 257
7. Jang YM , Seo JY , Chae KH , Yi M H , (2006) *Macrmol Res* 14(3) : 300
8. Mathews AS, Kim I, Ha CS , (2007) *Macromol Res* 15(2) : 114
9. Ogoshi T, Chujo Y, (2005) *Compos Interf* 11 : 539
10. Salomone JC, (1996) *Polymeric Materials Encyclopedia*, CRC Press, New York, 8 : 6253
11. Takeichi T, Tanikawa M, Zuo M, (1997) *J Polym Sci Part A: Polym Chem* 35 : 2395
12. Wahab MA, Kim I, Ha CS, (2003) *Polymer* 44 : 4705
13. Choi SW, Kim YK, Kim I, Ha CS, (2007) *J Appl Polym Sci* 103 : 2507
14. Im JS, Lee JH, An SK, Song KW, Jo NJ, Lee JO, Yoshinaga KJ, (2006) *J Appl Polym Sci* 100 : 2053
15. Zhu ZK, Yin J, Cao F, Shang XY, Lu QH, (2000) *Adv Mater* 12 : 1055
16. Cornelius CJ, Marand E, (2002) *Polymer* 43 : 2385
17. Kioul A, Mascia L, (1994) *J Non-Cryst Solids* 175 : 169
18. Kim Y, Lee WK, Cho WJ, Ha CS, Ree M, Chang T, (1997) *Polym Int* 43 : 129
19. Choi SW, (2006) M. S. Thesis, Pusan National University, Korea
20. Mascia L, Kioul A, (1995) *Polymer* 36 : 3649
21. Ha Y, Kim Y, Ha CS, (2008) *Polymer Bulletin* 59 : 833
22. Chang CC, Chen WC, (2002) *Chem Mater* 14 : 4242
23. Srinivasan SA, Hedrick JL, Miller RD, Di Pietro R, (1997) *Polymer* 38 : 3129
24. Glaser RH, Wilkes GL, Bronnimann CE, (1989) *J Non-Cryst Solids* 113 : 73
25. Joseph R, Zhang S, Ford WT, (1996) *Macromolecules* 29 : 1305
26. Young SK, Jarrett WL, Mauritz KA, (2002) *Polymer* 43 : 2311
27. Kim Y, (1996) Ph.D. Dissertation, Pusan National University, Korea.
28. Kim Y, Ree M, Chang T, Ha CS, Nunes TL, Lin LS, (1995) *J Polym Sci Part B: Polym Phys* 33 : 2075
29. Kim Y, Goh WH, Chang T, Ha CS, Ree M, (2004) *Adv Eng Mater* 6 : 39
30. Jeng U, Hsu CH, Lai YH, Chung WT, Shen HS, Lee HY, Song YF, Liang KS, Liu TL, (2005) *Macromol Res* 13(6) : 506
31. Russel TP, Brown HR, (1987) *J Polym Sci : Part B : Polym Phys* 25 : 1129
32. Ochi M, Takahashi R, (2001) *J Polym Sci : Part B : Polym Phys* 39 : 1071
33. Kweon JO, Noh ST, (2001) *J Appl Polym Sci* 81 : 2471